Journal of Solution Chemistry (2021) 50:503–516
https://doi.org/10.1007/s10953-021-01067-6

Effects of Water Content on Physicochemical Properties of a Protic Ionic Liquid with Monoprotic *N*-Hexylethylenediaminium as Cation and Bis(trifluoromethylsulfonyl) Imide as Anion

Er Hua[1,2,3] · **Zheng Liu**[1] · **Liling Qin**[1]

Received: 20 May 2020 / Accepted: 29 December 2020 / Published online: 1 April 2021

Abstract
The effects of water content on physicochemical properties such as density, dynamic viscosity, and electrical conductivity of HHexen(Tf_2N), composed of monoprotic *N*-hexylethylenediaminium as cation and bis(trifluoromethylsulfonyl) imide as anion, were studied in the temperature range $T = 303.15$–353.15 K. HHexen(Tf_2N) was dissolved a small amount of water (up to 6.53 wt%, corresponding to $w_0 = [H_2O]/[PIL] = 1.65$) as it is a hydrophobic protic ionic liquid (PIL). The physicochemical properties of HHexen(Tf_2N) were significantly influenced by its water content. The temperature dependence of the physicochemical properties at different water contents (0.50 wt%, 0.95%, 1.93%, 3.02%, 4.03%, 5.14% and 5.95%, corresponding to $w_0 = 0.12$, 0.23, 0.47, 0.74, 1.0, 1.28 and 1.50, respectively) were studied. With an increase in the water content, the density and dynamic viscosity decreases while the electric conductivity increases in a given temperature range. The Walden lines of HHexen(Tf_2N) show a good ionic character as the curves are all located in the range of $\Delta W = 0.5 \pm 0.2$ ($\Delta W = \log_{10} 1/\eta - \log_{10} \Lambda$) at different water contents. The ionicity shows an increasing trend with an increase of water content; this is evident when the water content rises to approximately 4.0% ($w_0 = 1.0$). Additionally, HHexen(Tf_2N) was used to extract Co(II) ions from an aqueous solution. Inductive coupled plasma emission spectrometry results showed that more than 99.5 wt% of Co(II) ions moved from the 100 mmol·kg^{-1} aqueous layer to the HHexen(Tf_2N) layer (of equal volume). After extraction of the Co(II) ions, the PIL layer contained 7.90% of water ($w_0 = 2.0$).

Keywords Protic ionic liquid · Water effect · Dynamic viscosity · Electric conductivity · Ionicity

✉ Er Hua
huaer0101@hotmail.com

[1] Chemical Science and Engineering College, North Minzu University, 204 Wenchang North Street, Xixia District, Yinchuan 750021, Ningxia, China

[2] Key Laboratory of Chemical Engineering and Technology, State Ethnic Affairs Commission, North Minzu University, 204 Wehchang North Street, Xixia District, Yinchuan 750021, Ningxia, China

[3] Ningxia Key Laboratory of Solar Chemical Conversion Technology, North Minzu University, 204 Wenchang North Street, Xixia District, Yinchuan 750021, Ningxia, China

1 Introduction

Ionic liquids (ILs) are molten salts in which the cations and anions are poorly coordinated. Hence, they exist as liquids at temperatures lower than 373 K or even at room temperature (i.e., room-temperature ILs (RTILs)) [1–4]. Ionic liquids are composed of relatively large asymmetric organic cations and inorganic or organic anions [5–7]. Room-temperature ILs are utilized at high temperatures as green solvents for organic reactions and as extraction solvents for transition metal ions, lubricants, or lubricant additives because of their good thermostability, non-volatility, and non-flammability [5, 8–10]. Ionic liquids are generally classified as either protic (PILs) and aprotic ILs (AILs). Aprotic ILs essentially consist of cations, which are not protonated, and counter anions. The key property that distinguishes PILs from other ILs is that PILs are formed via proton transfer from a Brønsted acid to a Brønsted base (Eq. 1) [11–13]. This leads to the presence of proton donor and acceptor sites, such that a hydrogen bond network is developed [14]. In this study, bis(trifluoromethylsulfonyl) imide acid (HTf_2N) was used as the Brønsted acid and hexylethylenediamine (Hexen) was the Brønsted base.

$$B + HA \rightleftharpoons HB^+ \cdot A^- \tag{1}$$

The HHexen(Tf_2N) studied here is a hydrophobic RT-PIL with a low melting point. The characteristic feature of this PIL (Scheme 1a) is that its cationic unit has the chelate ring moiety of ethylenediamine and thus it is advantageous for encapsulating transition metal ions, compared to monoamine-type PILs (Scheme 1b) [15, 16]. Therefore, in this study, the Co(II) extraction ability of HHexen(Tf_2N) from an aqueous solution was investigated. To identify the chelate effect on the incorporation of transition metal ions, an HHexam(Tf_2N) PIL (Scheme 1b) having hexylammonium (monoamine) as cation and bis(trifluoromethylsulfonyl) imide as anion was additionally used in an extraction experiment.

In general, PILs are more hydrophilic than AILs and, hence, tend to absorb water, which is generally difficult to eliminate. Occasionally, the water content has significant effects on the physicochemical properties of PILs, and it is important to investigate these influences [17]. As these PILs have the hydrophilic moiety of ethylenediamine, they can easily absorb water despite their macroscopic hydrophobicity. Hence, in the present study, the effects of water content on the physicochemical properties, such as density, dynamic viscosity, and electric conductivity for an HHexen(Tf_2N) PIL were studied in the temperature range of $T = 303.15$–353.15 K [11, 18].

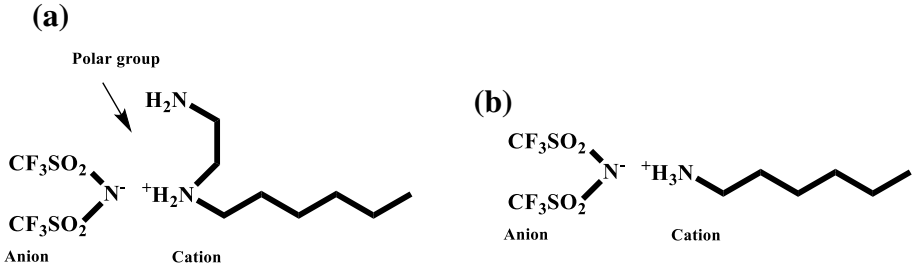

Scheme 1 Structures of **a** HHexen(Tf_2N) and **b** HHexam(Tf_2N)

2 Experimental Section

2.1 Materials

Ethylenediamine (> 99%, CAS 107-15-3, Tianjin Kemiou Chemical Reagent Co., Ltd.), *n*-hexylbromide (> 99%, CAS 111-25-1, Nanjing Duodian Chem. Co., Ltd.), and bis(trifluoromethylsulfonyl)imide acid (HTf_2N, > 99%, CAS 82113-65-3, Nanjing Duodian Chem. Co., Ltd.) were used as received. Diethyl ether (> 99.5%, CAS 60-29-7, Beijing Chemical Works) was treated in molecular sieves overnight and then distilled. Cobalt(II) chloride ($CoCl_2$, 98%, CAS 7646-79-9, Energy Chemical) was used as received.

2.2 Synthesis and Characterization of PILs

N-hexylethylenediamine was synthesised via the reaction between *n*-hexylbromide and ethylenediamine (molar ratio of 1:5) according to a procedure previously reported [19]. Monoprotic HHexen(Tf_2N) was synthesised via a simple neutralization reaction of the base, *N*-hexylethylenediamine, with the acid, HTf_2N (molar ratio of 1:1), in diethyl ether. The base and acid were mixed for 4 h and the product then isolated via the complete evaporation of diethyl ether, yielding HHexen(Tf_2N) as a pale yellowish, transparent liquid at room temperature, according to our previous work [11, 20]. The purity of HHexen(Tf_2N) was confirmed by ^{13}C-NMR spectra and CHN elemental analysis (see supplementary information).

HHexen(Tf_2N) was freeze-dried for 48 h at 223 K using an Alpha 1-2 LD plus freeze dryer (Martin Christ Freeze Dryers). Although we tried to remove the trace amounts of water to the extent possible, 0.50 wt% of water remained in the sample, which was designated as 'dried' HHexen(Tf_2N). The water contents of the water/PIL mixed solutions were determined using a V20 volumetric Karl Fischer titrator (Mettler Toledo).

2.3 Preparation of HHexen(Tf_2N) with Different Water Contents

The density, dynamic viscosity, and electric conductivity, of HHexen (Tf_2N) with an initial water content of 0.50 wt% were investigated in our previous study [11]. Similar investigations were carried out in the present study based on our previous work. The initial water content of HHexen (Tf_2N) in the present study was 0.50%. Firstly, the solubility of water in HHexen (Tf_2N) was examined and determined to be 6.53 wt%, although it is a hydrophobic PIL. The water/PIL systems were prepared with water contents of 1 wt%, 2%, 3%, 4%, 5%, and 6%. These water/PIL systems were mixed completely using a vortex mixer with adjustable speed prior to the experiments, and the water contents were confirmed using the V20 Karl Fischer titrator (Mettler Toledo). The water contents were measured to be 0.95 wt% (corresponding to $w_0 = [H_2O]/[PIL] = 0.23$, w_0: molar ratio of water to PIL), 1.93% ($w_0 = 0.47$), 3.02% ($w_0 = 0.74$), 4.03% ($w_0 = 1.0$), 5.14% ($w_0 = 1.28$), and 5.95% ($w_0 = 1.50$).

2.4 Density

Density values with the uncertainty of ± 0.0001 g·mL^{-1} were measured simply by measuring the weight of HHexen(Tf_2N) with different water contents filling a 1 mL volumetric Ostwald-type pycnometer in the temperature range of T = 303.15–353.15 K. The temperature was controlled by a thermostatic silicone oil bath with an accuracy of ± 0.1 K. The time to attain thermal equilibrium of the cell was approximately 30 min. [21].

2.5 Dynamic Viscosity

The dynamic viscosities of HHexen(Tf_2N) with different water contents were measured using a Lovis 2000 M micro-viscometer (Anton Paar) with a φ 1.8 mm glass capillary in the temperature range, T = 303.15–353.15 K. The Lovis 2000 M micro-viscometer has several advantages such as wide temperature range with an uncertainty of ± 0.1%, T = 243.15–373.15 K, and wide viscosity range with the uncertainty of ± 0.1%, 0.3–10,000 mPa·s. Prior to the measurements, the viscometer was calibrated using a standard calibration oil (APN415) provided by Paragon Scientific Ltd. The relationship between viscosity and density for the measurement is described as:

$$\eta = c\left(\rho_b - \rho_s\right)\Delta t, \tag{2}$$

where η is the dynamic viscosity, ρ_s and ρ_b are densities of HHexen(Tf_2N) and the steel ball, respectively, c is a constant, and Δt is the rolling time of the steel ball [21].

2.6 Electric Conductivity

The electric conductivities of HHexen(Tf_2N) with different water contents were measured using an electrical conductivity meter (Model DDS-11A, Leici Instrument, Shanghai, DJS-1. A cell with platinum black electrodes with cell constant of 0.985 cm^{-1}) was used for values in the order of magnitude of 0–10^3 μS·cm^{-1}; a Mettler Toledo Conductivity Measurement Instruments, Shanghai, the electrode Inlab 731 ISM with cell constant of 0.570 cm^{-1} was used for values in the order of magnitude of 10^3–10^4 μS·cm^{-1} and was calibrated by the calibration solution with 1413 μS·cm^{-1} [21]. The uncertainty for the measurement of the conductivity is ± 1.0%.

2.7 The Measurement of Co(II) Ion Concentration

The Co(II) ion concentration in the water layer was measured using an inductively coupled plasma spectrometer (model ICP-7000, Kingreid Ltd. Co., Beijing) under argon gas (purity ≥ 99.996%) as protecting gas at 80–90 psi, nitrogen gas (purity ≥ 99.999%) as flowing gas at 40 psi and as cutting gas at 70 psi; the temperature for the recycling water is 293 K. The accuracy of measurement for the metal concentration is 0.001 mg·L^{-1}. Calibration data for Co(II) ion are shown in the supplementary information.

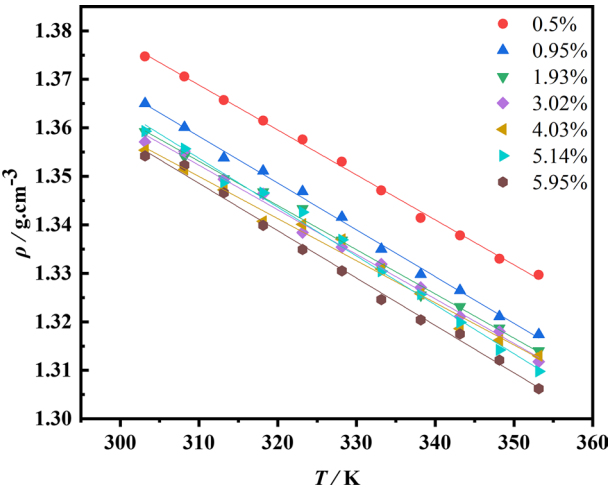

Fig. 1 Plots of ρ *vs.* temperature for HHexen (Tf_2N) with different water contents

3 Results and Discussion

3.1 Density

The density of HHexen(Tf_2N) decreases with an increase in water content and temperature (Fig. 1, data reported in Table S1). This may be because the denser packing of the HHexen(Tf_2N) PIL formed at lower water content and at lower temperature is destroyed by the hydration of each PIL ion and by raising of the temperature [22].

The experimental values of ρ were fitted using the following empirical equation, Eq. 3. The parameters obtained, i.e., b and α, and the correlation coefficient, R^2, are listed in Table 1 [23].

$$\rho = b + a \cdot T \tag{3}$$

In addition, the excess molar volumes V^{E} were calculated from the molar fractions, molar masses, and the densities of water, pure ionic liquid and the mixtures as given by Eq. 4:

$$V^{\mathrm{E}} = \frac{x_1 M_1 + x_2 M_2}{\rho_{12}} - \left(\frac{x_1 M_1}{\rho_1}\right) - \left(\frac{x_2 M_2}{\rho_2}\right) \tag{4}$$

where x_1 is the molar fraction of water, x_2 is molar fraction of PIL; ρ_{12}, ρ_1 and ρ_2 are the densities of the mixture, water and PIL, respectively. M_1 and M_2 are the relative molar masses for the water and PIL, respectively [24]. The excess molar volume is defined as

Table 1 Fitting parameters, i.e., α and b, and correlation coefficient R^2 from Eq. 3

Water content wt% (molar fraction of water x_1)	0.50% (0.11)	0.95% (0.19)	1.93% (0.32)	3.02% (0.42)	4.03% (0.50)	5.14% (0.56)	5.95% (0.60)
$10^4\ a/\mathrm{K}^{-1}$	− 9.2690	− 9.6436	− 9.1182	− 9.1873	− 8.6836	− 9.2691	− 9.7709
b	1.6562	1.6572	1.6358	1.6371	1.6192	1.6562	1.6515
R^2	0.9978	0.9968	0.9949	0.9946	0.9887	0.9949	0.9954

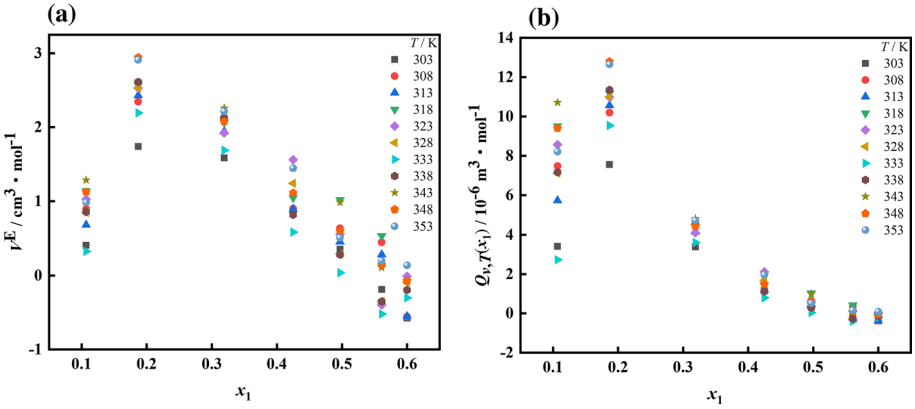

Fig. 2 Plots of **a** V^E and **b** $Q_{V,\exp,T}$ *vs.* molar fraction of water (x_1) at various temperatures

the difference between the ideal and the real molar volume, and the V^E value reflects the strength of the interaction between the different molecules.

Figure 2a (data are reported in Table S2a) shows that the value of V^E is the largest and positive at 0.95% (x_1: 0.19). This means that the interaction mode of the cation–anion–water ternary system changes at around $x_1 = 0.19$. There is a different interaction mode for the "dried" PIL (0.5%, $x_1 = 0.11$) system compared to the others. Negative values of V^E are only observed at higher water content.

Furthermore, the reduced Redlich and Kister function $Q_{V,\exp,T}$ gives a much better handle on the origin of the non-ideality than the direct excess property V^E. The relationship of $Q_{V,\exp,T}$ *vs.* x_1 is illustrated in Fig. 2b (Table S2b) [25].

$$Q_{V,\exp,T} = V^E / x_1 (1 - x_1) \tag{5}$$

It is remarkable that in the region from $x_1 = 0.11$ (0.5%, "dried") to $x_1 = 0.19$ both the V^E and $Q_{V,\exp,T}$ values increase with an increase in the water content. This indicates that the strong interaction between the cation and the anion at the lowest water content ($x_1 = 0.11$, i.e., "dried" condition) is loosened with an addition of small amounts of water by the hydration of the ions, which causes an increase in the molar volume of the contracted ion-pair structure of the dried PIL. The $Q_{V,\exp,T}$ values in Fig. 2b show a similar profile as that for V^E, whereas at higher water content, the dependence of $Q_{V,\exp,T}$ on the temperature and on the water content becomes significantly smaller with an increase in the water content. This trend and the monotonic decrease with an increase in the water content at around $x_1 > 0.2$ indicates that interstitial accommodation of water in the ion-pair network of PIL occurs and some stable hydration structures of the cation and the anion are formed.

3.2 Dynamic Viscosity

The dynamic viscosity of HHexen(Tf_2N) decreases with an increase in water content or temperature (Fig. 3a). The data are shown in Table S3 (see supplementary information). The viscosity of HHexen(Tf_2N) strongly depends on the water content. This is because the interactions between the cation and the anion are weakened by the hydration from an increase in the water content. In order to discuss the effect of cations on the viscosity

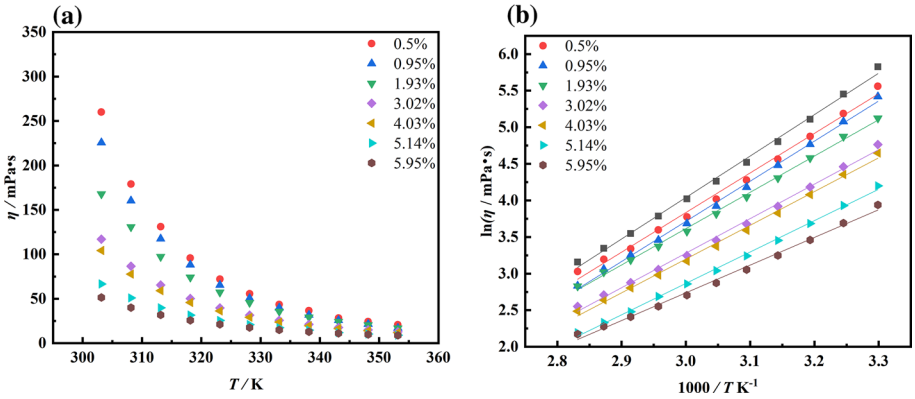

Fig. 3 **a** Viscosity of HHexen(Tf_2N) with different water contents as function of temperature, and **b** Arrhenius plots for viscosities

at the same water content, the viscosity of HHexen(Tf_2N) is compared with the case of HHexam(Tf_2N) studied in our previous work [26]. For these two PILs, the anion is the same and the polar groups are two amines and a mono-amine for HHexen(Tf_2N) and HHexam(Tf_2N), respectively. The results show that the effect of water on the viscosity is obvious for these two PILs and especially for the HHexam(Tf_2N) with the smaller mono-amine polar group. For example, the viscosity of HHexam(Tf_2N) is 45.4 mPa·s, about half of the 86.6 mPa·s for HHexen(Tf_2N) at $T = 308.15$ K and $w_0 = 0.74$. This is due to fact that the viscosity is governed by the size of PIL with increasing the water content [26].

The relationship between dynamic viscosity and temperature is usually fitted using the Arrhenius equation, Eq. 6 [27]:

$$\eta = \eta_\infty \exp(E_\eta / k_B T) \tag{6}$$

where E_η, η_∞, and k_B are the activation energy, maximum dynamic viscosity, and Boltzmann constant, respectively. The fitted parameters obtained are listed in Table 2. The ln η versus T^{-1} plot is presented in Fig. 3b. The relationship is almost linear and indicates that the viscosity of HHexen(Tf_2N) approximately follows the Arrhenius equation at different water contents (0.50–5.95%) in the temperature range of $T = 303.15$–353.15 K.

3.3 Electric Conductivity

The electric conductivity is generally governed by the mobility of the ions in the ILs, and correlates with viscosity, charge number, molecular weight, density, and ion size [4, 18]. The electric conductivity values of HHexen(Tf_2N) with different water contents in the

Table 2 Fitting parameters of E_η and correlation coefficient R^2 from Eq. 6

Water content (wt%)	0.50%	0.95%	1.93%	3.02%	4.03%	5.14%	5.95%
E_η/kJ·mol^{-1}	45	46	41	39	38	36	31
R^2	0.9937	0.9977	0.9980	0.9963	0.9966	0.9981	0.9946

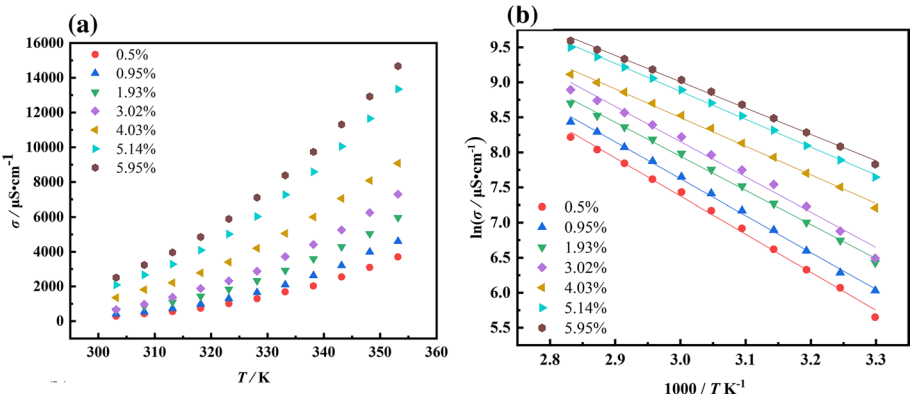

Fig. 4 **a** Conductivity of HHexen(Tf_2N) with different water contents as a function of temperature, and **b** Arrhenius plots for conductivities

temperature range of $T = 303.15–353.15$ K, are reported in supplementary Table S4. The electric conductivity (σ) is related to temperature, as plotted in Fig. 4, based on the Arrhenius equation, which is given as follows [28, 29]:

$$\sigma = \sigma_0 \exp\left(-E_\sigma / k_B T\right) \tag{7}$$

where E_σ, σ_0, and k_B are the activation energy, pre-exponential factor, and Boltzmann constant, respectively. The fitted parameters obtained are presented in Table 3. The relationship of ln σ *vs.* T^{-1} (Fig. 4b) shows that the linearity of the Arrhenius plot becomes better with an increase in water content [30]. At the same time, the value of E_σ (Table 3) is larger for the lower water content system and decreases with an increase of water content, since the ionic interaction in the ion-pair of PIL is stronger at lower water content compared to the water rich region.

The electric conductivity increases with the water content as observed for the decrease in the viscosity. These trends can be interpreted as follows. With an increase in the water content, the extent of hydration to the polar groups of the cation and of the anion increases; thus the motional restriction of the ions interacting with the counter ion is loosened, which leads to an enhancement of the mobility of ions.

In addition, by comparing with mono-amine type PIL of HHexam(Tf_2N) in our previous work [26], larger electric conductivity is observed for HHexam(Tf_2N) than for HHexen(Tf_2N) at the same water content. For example, the electrical conductivity of HHexam(Tf_2N) is 2480 μS·cm^{-1}, which is much larger than 972 μS·cm^{-1} for HHexen(Tf_2N) at $T = 308.15$ K and $w_0 = 0.74$. This difference can be interpreted as

Table 3 Fitting parameters of E_σ and correlation coefficient R^2 from Eq. 7

Water content (wt%)	0.50%	0.95%	1.93%	3.02%	4.03%	5.14%	5.95%
E_σ/kJ·mol^{-1}	45	44	40	42	34	33	31
R^2	0.9960	0.9978	0.9972	0.9887	0.9963	0.9985	0.9972

resulting from the larger size of HHexen(Tf_2N) than HHexam(Tf_2N) due to the double-amine headgroup [26].

3.4 Walden's Rule

The Walden rule has been extensively used to assess the ionicity of ILs. The relationship between molar conductivity and fluidity is described by the following Walden equation [31]:

$$\Lambda\eta = k \tag{8}$$

$$\log_{10}\Lambda = \log_{10}\eta^{-1} + \log_{10}k \tag{9}$$

where Λ, η, and k are the molar conductivity, dynamic viscosity, and a temperature-dependent constant, respectively. In particular, the Walden rule represents a qualitative approach to investigating the 'ionicity' of ILs [32]. The position of the ideal line was established using an aqueous KCl solution at high dilution [33]. The molar conductivity (Λ) was calculated using the following equation and data are reported in Table S5):

$$\Lambda = \sigma \cdot M \cdot \rho^{-1}, \tag{10}$$

where Λ, σ, M, and ρ are the molar conductivity, electric conductivity, molar mass, and density, respectively. The Walden plots are described by the relationship between $\log_{10}\Lambda$ and $\log_{10}\eta^{-1}$ (Fig. 5). The Walden lines are approximately straight lines and the slopes are in the range of 1.0 ± 0.1 for the water content range of 0.50–5.95%. They present a good ionic character as the curves are all located in the range of $\Delta W = 0.5 \pm 0.2$ ($\Delta W = \log_{10}1/\eta - \log_{10}\Lambda$) [34]. The ionicity shows an increasing trend with an increase of water content. This trend is evident when the water content rises to approximately 4.0% ($w_0 = 1.0$). Furthermore, it is characteristic that at the lowest water content (0.5%). the dynamic property ΔW has a value less than 0.5. This result is consistent with the other physical properties such as V^E (Fig. 2a) and the Arrhenius plot for $\ln\sigma$ (Fig. 4b), where the lowest water

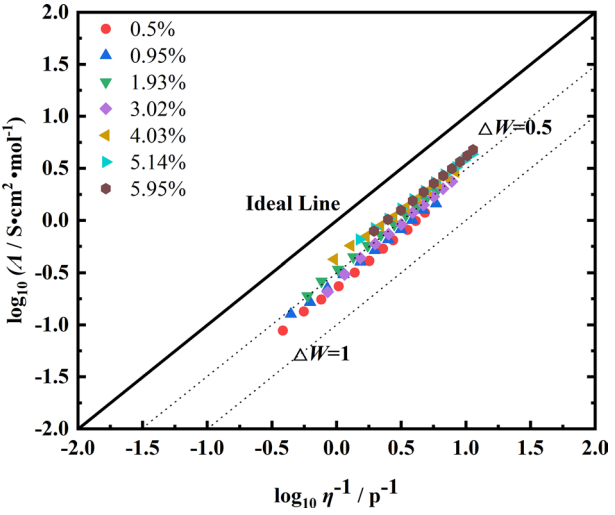

Fig. 5 Walden plots for HHexen(Tf_2N) with different water contents in the temperature range of $T = 303.15$–353.15 K

content (0.5%) system indicates stronger ionic interactions in the ion-pair of PIL compared to the other water richer systems.

3.5 Extraction of Co(II) Ions

3.5.1 Extraction Process

Additionally, as an application study, the hydrophobic HHexen(Tf_2N) PIL was used to extract Co(II) ion from a 100 mmol·kg^{-1} $CoCl_2$ aqueous solution, since there are chelate amines in the polar group of this IL. For the extraction experiment, equal volumes (0.4 mL: 0.4 mL) of the aqueous $CoCl_2$ solution and HHexen(Tf_2N) PIL were mixed (Scheme 2a middle: upper layer for aqueous Co(II) ion phase and lower phase for pure HHexen(Tf_2N)). The mixed solution immediately separated into a colorless aqueous layer and clarlet colored HHexen(Tf_2N) layer (Scheme 2a right: Co(II) ions were extracted by the HHexen(Tf_2N) layer).

Then, 0.16 mL of solution was removed from the aqueous layer and diluted to the 25 mL in a volumetric flask. Finally, 1 mL of the diluted solution was prepared to measure the concentration of Co(II) ion; the concentration measured was 0.003 mg·L^{-1}.

For comparison, HHexam(Tf_2N), the hexylmonoamine derivative was used to extract Co(II) ions from its aqueous solution under the same conditions. However, no Co(II) ions were transferred to the PIL layer. (Scheme 2c).

3.5.2 Solubility of Co(II) Salt in PIL

The Co(II) ion concentration of the water layer after the extraction by the PIL was measured using inductive coupled plasma emission spectrometry (the data of calibration curve is shown in supporting information). The result showed that more than 99.5% of Co(II) ions were transferred from the 100 mmol·kg^{-1} aqueous layer to HHexen(Tf_2N). This suggests that HHexen(Tf_2N) can extract $CoCl_2$ from its aqueous solution at high rate. In contrast, HHexam(Tf_2N) could not extract Co(II) ions from the aqueous solution under the same conditions and their color remained unchanged. This is because hexylammonium is a monoamine and has no chelating effect on the extraction. On the other hand, a characteristic of HHexen(Tf_2N) is having a chelate ring (ethylenediamine) moiety; thus it is advantageous to encapsulate transition metal ions, i.e., some Co(II) complex is formed (Scheme 2b). Therefore, the PIL with the chelating amine has an advantage to encapsulate Co(II) ions compared to the monoamine type PIL.

3.5.3 Water Content

The water content of the Co(II)/HHexen(Tf_2N) layer was determined to be $w_0 = 2.0$ (7.90%). This is higher than the maximum water content of pure HHexen(Tf_2N) (6.53%, $w_0 = 1.65$). This may be due to the fact that the Co(II) complex is formed in the Co(II)/HHexen(Tf_2N) layer and it contains two water molecules. This suggests that the incorporation of the Co(II) ion leads to the formation of the $Co(H_2O)_2(Hexen)_2$ complex in the PIL layer.

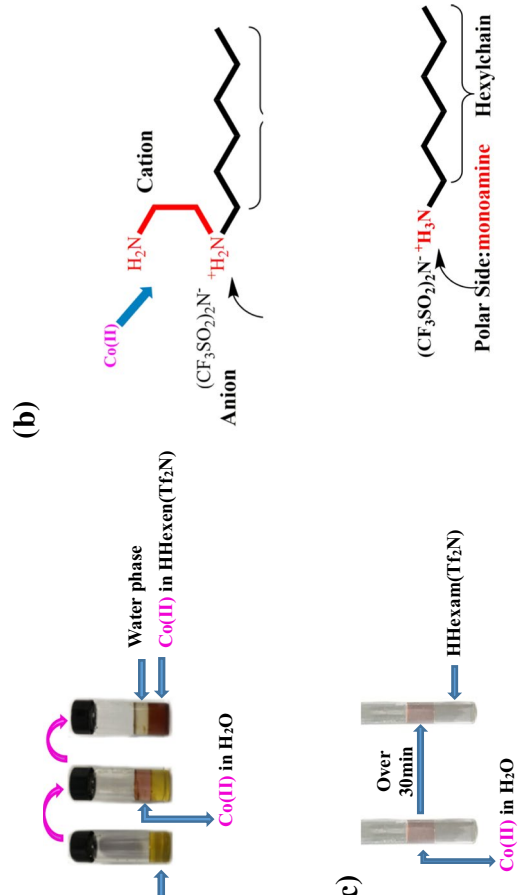

Scheme 2 **a** The image of extraction process using HHexen(Tf_2N) from aqueous Co(II) solution and **b** Co(II) ion encapsulation mechanism; **c** image of aqueous Co(II) solution separating with HHexam(Tf_2N)

4 Conclusion

Water dissolves in HHexen(Tf_2N) up to the extent of 6.53%, despite HHexen(Tf_2N) being a hydrophobic PIL. The effects of water content on the physicochemical properties of hydrophobic HHexen(Tf_2N) have been studied and shown to be interesting. The ion-pair structure of dried (water content 0.50 wt%, $w_0 = 0.12$) PIL is significantly changed with an addition of a small amount (0.95%, $w_0 = 0$) of water. The Walden lines of HHexen(Tf_2N) are all located in the range of $\Delta W = 0.5 \pm 0.2$. The ionicity increases with an increase of water content and this trend is evident up to approximately $w_0 = 1.0$. The inductive coupled plasma emission spectrometry shows that more than 99.5% of the Co(II) ions move from the 100 $mmol \cdot kg^{-1}$ aqueous layer to the HHexen(Tf_2N) PIL layer, and the water content of the Co(II)/HHexen(Tf_2N) PIL is $w_0 = 2.0$, suggesting the formation of the $Co(H_2O)_2(Hexen)_2$ complex in the PIL layer. In contrast, HHexam(Tf_2N) could not extract Co(II) ions from the aqueous solution under the same conditions.

Supplementary Information The online version contains supplementary material available at https://doi.org/10.1007/s10953-021-01067-6.

Acknowledgements This work was financially supported by the Foundation of Ningxia Higher Education (Project Number: NGY2020063). We are also grateful to Prof. Masayasu Iida of Nara Women's University for the helpful discussion. We would like to thank Editage (www.editage.com) for English language editing.

Declarations

Conflict of interest The authors declare that they have no conflict of interest.

References

1. Patil, A.B., Mahadeo, B.B.: Brønsted acidity of protic ionic liquids: a modern ab initio valence bond theory perspective. Phys. Chem. Chem. Phys. **18**, 26020–26025 (2016)
2. Piekart, J., Łuczak, J.: Transport properties of aqueous ionic liquid microemulsions: influence of the anion type and presence of the co-surfactant. Soft Matter **11**, 8992–9008 (2015)
3. Ullah, Z., Bustam, M.A., Man, Z., Muhammad, N., Khan, A.S.: Synthesis, characterization and the effect of temperature on different physicochemical properties of protic ionic liquids. RSC Adv. **5**, 71449–71461 (2015)
4. Jacquemin, J., Husson, P., Padua, A.A.H., Majer, V.: Density and viscosity of several pure and water-saturated ionic liquids. Green Chem. **8**, 172–180 (2006)
5. Cohen, D.T., Zhang, C., Fadzen, M., Mijalis, A.J., Hie, L., Johnson, K.D., Shriver, Z., Plante, O., Miller, S.J., Buchwald, S.L., Pentelute, B.L.: A chemoselective strategy for late-stage functionalization of complex small molecules with polypeptides and proteins. Nat. Chem. **11**, 78–85 (2019)
6. Singh, A.P., Gardas, R., Senapati, S.: How water manifests the structural regimes in ionic liquids. Soft Matter **13**, 2348–2361 (2017)
7. He, Z., Alexandridis, P.: Nanoparticles in ionic liquids: interactions and organization. Phys. Chem. Chem. Phys. **17**, 18238–18261 (2015)
8. Wippermann, K., Giffin, J., Kuhri, S., Lehnert, W., Korte, C.: The influence of water content in a proton-conducting ionic liquid on the double layer properties of the Pt/PIL Interface. Phys. Chem. Chem. Phys. **19**, 24706–24723 (2017)
9. Singh, A.P., Gardas, R., Senapati, S.: Divergent trend in density versus viscosity of ionic liquid/water mixtures: a molecular view from guanidinium ionic liquids. Phys. Chem. Chem. Phys. **17**, 25037–25048 (2015)

10. Walst, K.J., Yunis, R., Bayley, P.M., MacFarlane, D.R., Ward, C.J., Wang, R., Curnow, O.J.: Synthesis and physical properties of tris(dialkylamino)cyclopropenium bistriflamide ionic liquids. RSC Adv. **5**, 39565–39579 (2015)
11. Er, H., Xu, Y., Zhao, H.: Properties of mono-protic ionic liquids composed of hexylammonium and hexylethylenediaminium cations with trifluoroacetate and bis(trifluoromethylsulfonyl) imide anions. J. Mol. Liq. **276**, 379–384 (2019)
12. Walden, P.: Molecular weights and electrical conductivity of several fused salts. Bull. Acad. Sci. St. Petersburg **1800**, 405–422 (1914)
13. Greaves, T.L., Drummond, C.J.: Protic ionic liquids: properties and applications. Chem. Rev. **108**, 206–237 (2008)
14. Kellkar, M.S., Maginn, E.J.: Effect of temperature and water content on the shear viscosity of the ionic liquid 1-ethyl-3-methylimidazolium bis(trifluoromethanesulfonyl)imide as studied by atomistic simulations. J. Phys. Chem. B **18**, 4867–4876 (2007)
15. Takemura, S., Kawakami, S., Harada, M., Iida, M.: Solvation structure of a copper(II) ion in protic ionic liquids comprising *N*-hexylethylenediamine. Inorg. Chem. **53**, 9667–9678 (2014)
16. Watanabe, M., Nakayama, C., Yasuda, H., Harada, M., Iida, M.: Interactions of nickel(II) ions in protic ionic liquids comprising *N*-hexyl(or *N*-2-ethtylhexyl)ethylenediamines. J. Mol. Liq. **214**, 77–85 (2016)
17. Grishina, E.P., Ramenskaya, L.M., Gruzdev, M.S., Kraeva, O.V.: Water effect on physicochemical properties of 1-butyl-3-methylimidazolium based ionic liquids with inorganic anions. J. Mol. Liq. **117**, 267–272 (2013)
18. Watanabe, M., Takemura, S., Kawakami, S., Syouno, E., Kurosu, H., Harada, M., Iida, M.: Sites of protonation and copper(II) complexation in protic ionic liquids comprised of *N*-hexylethylenediaminium cation. J. Mol. Liq. **183**, 50–58 (2013)
19. Bruno, A.J., Chaberek, S., Martell, A.E.: The preparation and properties of *N*-substituted ethylenediaminetriacetic acids. J. Am. Chem. Soc. **12**, 2723–2728 (1956)
20. Iida, M., Kawakami, S., Syouno, E.: Hua, Er: properties of ionic liquids containing silver(I) or protic alkylethylenediamine cations with a bis(trifluoromethanesulfonyl) amide anion. J. Colloid Interface Sci. **356**, 630–638 (2011)
21. Er, H., Wang, H.: Properties of protic ionic liquids composed of *N*-alkyl (= hexyl, octyl and 2-ethylhexyl) ethylenediaminum cations with trifluoromethanesulfonate and trifluoroacetate anion. J. Mol. Liq. **220**, 649–656 (2016)
22. Dupont, J.: On the solid, liquid and solution structural organization of imidazolium ionic liquids. J. Braz. Chem. Soc. **15**, 341–350 (2004)
23. Zhang, Q.G., Li, Q., Liu, D., Zhang, X.Y., Lang, X.S.: Density, dynamic viscosity, electrical conductivity, electrochemical potential window, and excess properties of ionic liquid *N*-butyl-pyridinium dicyanamide and binary system with propylene carbonate. J. Mol. Liq. **249**, 1097–1106 (2018)
24. Oswal, S.L., Desai, H.S.: Studies of viscosity and excess molar volume of binary mixtures 2. Butylamine + 1-alkanol mixtures at 303.15 and 313.15 K. Fluid Phase Equilib. **161**, 191–204 (1999)
25. Das, D., Messaâdi, A., Barhoumi, Z., Ouerfelli, N.: The relative reduced Redlich–Kister equations for correlating excess properties of *N*,*N*-dimethylacetamide + water binary mixtures at temperatures from 298.15 K to 318.15 K. J. Solution Chem. **41**, 1555–1574 (2012)
26. Liu, Z., Hua, Er, Liu, R., Ji, J.L.: Water effects on physicochemical properties of protic ionic liquid with N-hexylamine as cation and bis(trifluoromethylsulfonyl) imide as anion. Chem. Ind. Eng. Prog. (2020). https://doi.org/10.16085/j.issn.1000-6613.2020-0940
27. Xu, W., Cooper, E.I., Angell, C.A.: Ionic liquids: ion mobilities, glass temperatures, and fragilities. J. Phys. Chem. B **25**, 6170–6178 (2003)
28. Xu, W., Angell, C.A.: Solvent-free electrolytes with aqueous solution-like conductivities. Science **302**, 422–425 (2003)
29. Liu, Q.S., Liu, J., Liu, X.X., Zhang, S.T.: Density, dynamic viscosity, and electrical conductivity of two hydrophobic functionalized ionic liquids. J. Chem. Thermodyn. **90**, 39–45 (2015)
30. Schreiner, C., Zugmann, S., Hartl, R., Gores, H.J.: Fractional Walden rule for ionic liquids: examples from recent measurements and a critique of the so-called ideal KCl line for the Walden plot. J. Chem. Eng. Data **5**, 1784–1788 (2010)
31. Iida, M., Baba, C., Inoue, M., Yoshida, H., Taguchi, E., Furusho, H.: Ionic liquids of bis(alkylethylenediamine)silver(I) salts and the formation of silver(0) nanoparticles from the ionic liquid system. Chem. Eur. J. **14**, 5047–5056 (2008)
32. MacFarlane, D.R., Forsyth, M., Izgorodin, E.I.A., Abbot, A.P., Annat, G., Fraser, K.: On the concept of ionicity in ionic liquid. Phys. Chem. Chem. Phys. **11**, 4962–4967 (2009)

33. Liu, Q.S., Li, P.P., Welz-Biermann, U., Chen, J., Liu, X.X.: Density, dynamic viscosity and electrical conductivity of pyridinium-based hydrophobic ionic liquids. J. Chem. Thermodyn. **66**, 88–94 (2013)
34. Yoshizawa, M., Xu, W., Angell, C.A.: Ionic liquids by proton transfer: vapor pressure, conductivity, and the relevance of ΔpKa from aqueous solutions. J. Am. Chem. Soc. **125**, 15411–15419 (2003)